

Homogeneous Catalysis

Mechanistic Investigation of Molybdate-Catalysed Transfer Hydrodeoxygenation

Daniel B. Larsen⁺, Allan R. Petersen⁺, Johannes R. Dethlefsen, Ayele Teshome, and Peter Fristrup^{*[a]}

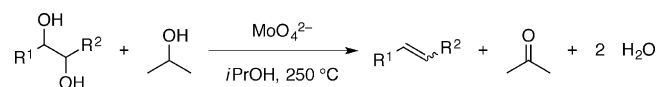
Abstract: The molybdate-catalysed transfer hydrodeoxygenation (HDO) of benzyl alcohol to toluene driven by oxidation of the solvent isopropyl alcohol to acetone has been investigated by using a combination of experimental and computational methods. A Hammett study that compared the relative rates for the transfer HDO of five *para*-substituted benzylic alcohols was carried out. Density-functional theory (DFT) calculations suggest a transition state with significant loss of aromaticity contributes to the lack of linearity

observed in the Hammett study. The transfer HDO could also be carried out in neat PhCH₂OH at 175 °C. Under these conditions, PhCH₂OH underwent disproportionation to yield benzaldehyde, toluene, and significant amounts of bibenzyl. Isotopic-labelling experiments (using PhCH₂OD and PhCD₂OH) showed that incorporation of deuterium into the resultant toluene originated from the α position of benzyl alcohol, which is in line with the mechanism suggested by the DFT study.

Introduction

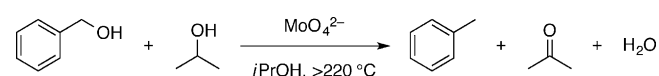
The production of organic platform chemicals from renewable feedstocks requires the development of reactions capable of reducing the oxygen content of biomass. A particularly abundant motif in biomass is the hydroxy group, and an emerging strategy to transform vicinal diols into the corresponding alkenes in a single step is the deoxydehydration (DODH) reaction, which typically involves the use of a rhenium-,^[1–6] molybdenum-,^[7–10] or vanadium-based^[11] catalyst. We have recently shown^[10] that the molybdate ion, prepared in situ by the addition of a slight excess of Bu₄NOH to a solution of [(NH₄)₆Mo₇O₂₄]·4H₂O (AHM), catalyses the DODH reaction of aliphatic diols in *i*PrOH, which serves as both the solvent and reductant (Scheme 1).

In addition, it was discovered that aldehydes and ketones underwent transfer hydrogenation to the corresponding mon-



Scheme 1. Molybdate-catalysed DODH reaction of a vicinal diol into an alkene driven by the oxidation of *i*PrOH to acetone.

ohydric alcohols. Interestingly, it was also discovered that allylic and benzylic alcohols underwent transfer hydrodeoxygenation (HDO), exemplified by the transfer HDO of benzyl alcohol to toluene in a yield of 93 % (Scheme 2).



Scheme 2. Molybdate-catalysed transfer HDO of benzyl alcohol into toluene driven by the oxidation of *i*PrOH to acetone.

The traditional hydrogenation and HDO reactions, as well as the other hydrotreatment reactions of hydrodenitrogenation (HDN), hydrodesulfurisation (HDS), and hydrodemetallation (HDM), are employed to remove heteroatoms from fossil resources and saturate double bonds to produce high-quality fuels with good stability.^[12,13] For biomass, the removal of oxygen is by far the most important reaction. Consequently, the catalytic upgrading of bio-oil, obtained from the pyrolysis of biomass, by means of the HDO reaction has been extensively reviewed.^[14–16] Most research has focused on complete HDO and hydrogenation, in which the products are ultimately alkanes that are suitable biofuels. On the contrary, the production of biomass-derived chemicals requires the removal of oxygen and the preservation of some functionality; therefore, complete HDO with concomitant hydrogenation is not desirable.

The catalysts typically employed in the HDO of biomass are based on noble metals, for example, platinum,^[17] ruthenium,^[18] palladium,^[19] or rhenium,^[20] and the products have been alkanes. The hydrogenation of double bonds can, however, be avoided if non-noble metals are used; for example, MoO₃ catalyses the HDO of acetone to propylene,^[21] tungsten oxides (in

[a] D. B. Larsen,⁺ Dr. A. R. Petersen,⁺ Dr. J. R. Dethlefsen, Dr. A. Teshome, Dr. P. Fristrup
Department of Chemistry, Technical University of Denmark
Kemitorvet 207, 2800 Kgs. Lyngby (Denmark)
E-mail: pf@kemi.dtu.dk

[⁺] These authors contributed equally to this work.

Supporting information for this article is available on the WWW under <http://dx.doi.org/10.1002/chem.201603028>.

combination with Pd) catalyse the transformation of a cyclic vicinal diol into a cyclic monohydric alcohol,^[22] and FeS₂ catalyses the HDO (or hydrogenolysis) of dibenzyl ether to toluene.^[23] The suppression of the hydrogenation by the addition of a non-noble metal has been illustrated by Abu-Omar and co-workers, who showed that the addition of ZnCl₂ in the Pd-catalysed HDO of the carbohydrate-derived platform molecule 5-(hydroxymethyl)furfural^[25] prevented the hydrogenation of carbon-carbon double bonds.^[25] Herein, we present an alternative “transfer HDO” pathway catalysed by molybdate ions, which was discovered as a minor side reaction during the DODH of vicinal diol. Although the reaction has shown promising results in the conversion of allyl alcohol into propylene and 1,5-hexadiene, it is clear that a more efficient protocol must be developed for the reaction to obtain widespread use. To this end, we have carried out a mechanistic study of the Mo-catalysed transfer HDO that uses the deoxygenation of benzyl alcohol to toluene as a convenient model reaction. The reactivities of other functional groups (i.e., carbonyl compounds, acetals, ethers, amines, and thiols) were also screened.

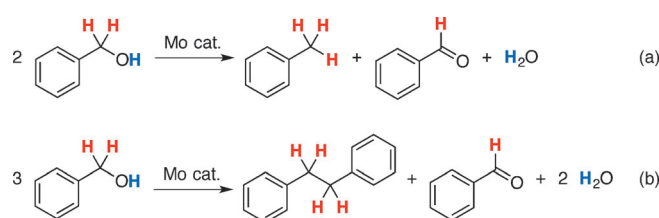
Computational studies allowed for the proposal of a mechanism, which was corroborated by a combined computational and experimental Hammett study. Furthermore, deuterium-labelling studies were employed to ascertain deuterium incorporation into the products and the change in the product distribution.

Results and Discussion

Disproportionation of neat benzyl alcohol

Akin to our previous study of DODH of 1,2-hexanediol, we hypothesised that PhCH₂OH could disproportionate.^[8] Consequently, transfer HDO could be carried out under neat conditions and yield equimolar amounts of toluene and benzaldehyde (Scheme 3a).

PhCH₂OH (1.51 g) and [(Bu₄N)₂Mo₆O₁₉] (21.2 mg, 0.67 mol% of Mo) were heated to 220 °C in a microwave reactor for 3 hours. The three products toluene, bibenzyl, and benzaldehyde and starting-material benzyl alcohol were identified by means of GC and GC-MS (Table 1, entry 1).^[26] The sum of the relative molar amounts of toluene and bibenzyl should equal the relative molar amount of benzaldehyde, but due to the



Scheme 3. Molybdenum-catalysed disproportionation of benzyl alcohol to benzaldehyde and a) toluene, or b) bibenzyl.

presence of other minor by-products (“tribenzyl” and “tetra-benzyl”), this value was somewhat lower. The byproduct bibenzyl presumably forms according to Scheme 3b; even though two molecules of PhCH₂OH end up in bibenzyl, only one molecule of PhCH₂OH needs to be oxidised. The formation of the coupled bibenzyl product has also been observed when employing a rhenium catalyst, which was suggested to be the result of the formation of benzyl radicals that undergo coupling.^[26]

Deuterium-labelling experiments were carried out to gain further mechanistic insight. Separate experiments with PhCH₂OD and PhCD₂OH indicate where the hydrogen atoms end up in the products. By using PhCH₂OD, no deuterium atoms were incorporated in any of the products (Table 1, entry 2; GC-MS in the Supporting Information) and the relative molar amounts of the four components were essentially unchanged. PhCD₂OH, on the other hand, resulted in a significantly higher relative amount of bibenzyl relative to toluene (Table 1, entry 3). This outcome may suggest that the stronger C–D bond prevents the formation of toluene. The toluene formed was PhCD₃, the benzaldehyde was PhCDO, and the bibenzyl was PhCD₂CD₂Ph (confirmed by GC-MS; see the Supporting Information).

In two competition experiments, equimolar amounts of PhCH₂OH or PhCD₂OH were mixed with *para*-methylbenzyl alcohol. The experiment with PhCD₂OH had significantly more remaining starting material (31 vs. 16% PhCH₂OH), thus indicating a kinetic isotope effect (KIE) of greater than 1, which is indicative of C–H/D bond breakage in the rate-determining step (Table 1, entries 4 and 5). Although deuterium incorporation in the products was observed by GC-MS analysis, attempts to distinguish the different isotopologues of toluene and

Table 1. Product distributions obtained in the disproportionation of benzyl alcohol and deuterium-labelled benzyl alcohol at 220 °C.^[a]

Reactant	Toluene [%]	Bibenzyl [%]	Benzaldehyde [%]	Benzyl alcohol [%]
PhCH ₂ OH	28	6	39	28
PhCH ₂ OD	31	7	39	24
PhCD ₂ OH	17	16	36	32
PhCH ₂ OH/ <i>p</i> -MePhCH ₂ OH ^[b]	35/38	8/10	41/44	16/8
PhCD ₂ OH/ <i>p</i> -MePhCH ₂ OH ^[b]	30/40	9/8	30/44	31/9
PhCH ₂ OH ^[c]	35	5	39	20
PhCH ₂ OH ^[d]	40	8	44	9

[a] Unless otherwise noted, a total of 1.5 g of reactant and 0.7 mol% of [(Bu₄N)₂Mo₆O₁₉] were heated to 220 °C for 3 h in a microwave oven. [b] For *para*-MePhCH₂OH, the four major compounds were xylene, 1,2-di-*para*-tolylethane, *para*-methylbenzaldehyde, and *para*-methylbenzyl alcohol. [c] Heated to 200 °C for 6 h. [d] Heated to 240 °C for 2 h.

xylene proved inconclusive. Consequently, attention was turned to the bibenzyl species. Only three bibenzyl species were detected, namely, $\text{PhCD}_2\text{CD}_2\text{Ph}$, $p\text{-MePhCH}_2\text{CD}_2\text{Ph}$, and $p\text{-MePhCH}_2\text{CH}_2p\text{-MePh}$ (confirmed by GC-MS; see the Supporting Information), thus suggesting that H/D scrambling after the carbon-carbon bond-forming step does not occur.

To study the effect of temperature on the product distribution, the aforementioned disproportionation of neat PhCH_2OH was repeated at intervals of 10°C between 200 and 240°C . The reaction was slower at 200°C , but the product distribution after 6 hours was similar to the distribution obtained at 220°C after 3 hours (Table 1, compare entries 1 and 6). When the reaction was run at 240°C for 2 hours, the product distribution was not significantly affected, but the conversion was higher (Table 1, compare entries 1 and 7). This finding indicates that the formation of bibenzyl is not affected by entropy to an extent that could be expected for dimerisation.

Use of *i*PrOH as the solvent

As we previously have reported, *i*PrOH was suitable as the solvent and reductant.^[10] The $[\text{MoO}_4]^{2-}$ -catalysed transfer HDO of PhCH_2OH to toluene at $240\text{--}250^\circ\text{C}$ was conducted in *i*PrOH. To follow the reaction progress, samples were taken out during the course of the reaction. Starting with 100 mmol of PhCH_2OH and 0.358 mol% AHM (2.5 mol% with respect to Mo), the temporal evolution of the concentrations of PhCH_2OH , PhCH_3 , and PhCHO was plotted (Figure 1). The heating plate was turned on at $t=0$, the temperature reached 230°C after 40 minutes, and the reaction was complete within 3 h (see Figure S2 in the Supporting Information for the heating profile). When starting with 100 mmol of PhCH_2OH in 200 mL of *i*PrOH, some PhCHO was produced and was subsequently reduced as the reaction progresses. For the first few cycles, PhCH_2OH would compete with *i*PrOH for the role as the reductant and some disproportionation took place. A slower reaction with complete conversion of PhCH_2OH within 4 hours resulted by substituting EtOH for *i*PrOH as the solvent and reductant (see Figure S3 in the Supporting Information).

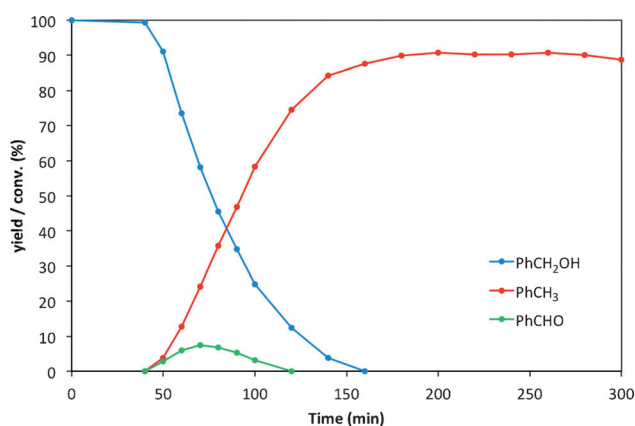


Figure 1. Temporal evolution of the concentrations of benzyl alcohol, toluene, and benzaldehyde.

To assess the nuclearity of the active catalytic species, the monomolybdate $[(\text{Bu}_4\text{N})_2\text{MoO}_4]$ and polymolybdate $[(\text{Bu}_4\text{N})_2\text{Mo}_6\text{O}_{19}]$ species were tested as catalysts for the HDO of benzyl alcohol. With catalyst loadings of 2.5 and 0.417 mol% for $[(\text{Bu}_4\text{N})_2\text{MoO}_4]$ and $[(\text{Bu}_4\text{N})_2\text{Mo}_6\text{O}_{19}]$ (2.5 mol% with respect to Mo), respectively, the two catalysts performed near identically (see Figure S4 in the Supporting Information). Interestingly, the two catalysts performed slightly faster than AHM (see Figure S5 in the Supporting Information). Consequently, when $[(\text{Bu}_4\text{N})_2\text{MoO}_4]$ or $[(\text{Bu}_4\text{N})_2\text{Mo}_6\text{O}_{19}]$ was used, the 100 mmol of benzyl alcohol were consumed within 140 minutes relative to 160 minutes when AHM was employed. This difference is attributed to the slow onset of the reaction between AHM and Bu_4NOH due to the poor solubility of AHM in *i*PrOH.

The near identical reactivities of $[(\text{Bu}_4\text{N})_2\text{MoO}_4]$ and $[(\text{Bu}_4\text{N})_2\text{Mo}_6\text{O}_{19}]$ suggest that the two catalysts have the same active catalytic species. Polymolybdates are usually obtained from weakly acidic solutions, whereas the Mo^{VI} ion is present as the $[\text{MoO}_4]^{2-}$ ion in strongly alkaline solutions. Given that AHM was used with the addition of Bu_4OH , it is proposed that a monomolybdate species similar to $[(\text{Bu}_4\text{N})_2\text{MoO}_4]$ is the active catalytic species.

By using 100 mmol of benzyl alcohol and varying the amount of AHM, reactions were conducted with catalyst loadings of 0.5, 1.0, 2.5, and 5.0 mol% with respect to Mo (Figure 2). As expected, an increase in the catalyst loading led to a faster consumption of PhCH_2OH . A plot of the log of the initial rate of toluene formation ν_0 against the log of the concentration of molybdenum gave a partial order with respect to molybdenum of 0.4 (see Figure S6 in the Supporting Information).

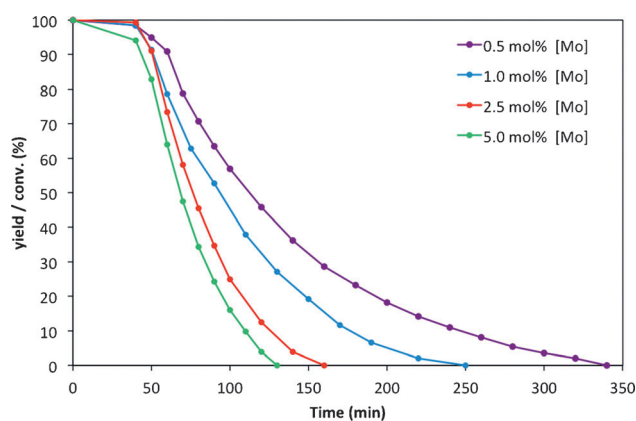


Figure 2. Temporal evolution of the concentration of benzyl alcohol while varying the catalyst loading.

By starting with 8 mmol of benzyl alcohol, the reaction order with respect to molybdenum was also investigated at a low substrate concentration. Reactions were conducted that used AHM loadings of 1.0, 2.5, 5.0, and 7.5 mol% with respect to Mo (see Figure S7 in the Supporting Information). The partial order of molybdenum was determined to be 1.0. When plotting $\ln\{[\text{PhCH}_2\text{OH}]/[\text{PhCH}_2\text{OH}]_0\}$ against time for the reac-

tion with 1.0 mol% Mo, a straight line was obtained that corroborates that the reaction is first order with respect to molybdenum (see Figures S8 and S9 in the Supporting Information). The divergence in the partial order of molybdenum, observed for high and low benzyl alcohol concentrations, is attributed to the aforementioned disproportionation of benzyl alcohol at high concentration.

Dilution experiments were carried out by varying the starting concentrations of PhCH₂OH, yet leaving the ratio of PhCH₂OH/AHM constant. Hence, the required catalyst turnover number to reach full conversion remained unchanged. Reactions starting with 50, 20, 8, and 4 mmol of PhCH₂OH were followed over time (see Figure S10 in the Supporting Information). The effect of diluting the reaction mixture became apparent when using 8 and 4 mmol of substrate, for which the consumption of PhCH₂OH slowed and the formation of PhCHO was no longer observed.

A deuterium-labelling experiment was conducted to ascertain the role of disproportionation during the reaction. The transfer HDO reaction of 50 mmol of PhCD(OH)CH₃ was subjected to the standard reaction conditions in *i*PrOH. Significant disproportionation would result in scrambling of the deuterium atom in the α position, thus leading to the products PhCHDCH₃, PhCH₂CH₃, and PhCD₂CH₃. Nevertheless, the major product was always PhCHDCH₃, and minor products α -[D₁]-styrene, (1-deutero-1-isopropoxyethyl)benzene, and *meso*- and *rac*-2,3-bideutero-2,3-diphenylbutane were also detected. This outcome excludes the possibility that a significant proportion of the benzylic alcohol undergoes disproportionation to ethylbenzene and acetophenone with concomitant transfer hydrogenation of acetophenone to 1-phenylethanol and subsequent HDO to ethylbenzene. On this basis, we conclude that the main reaction is a transfer HDO that involves *i*PrOH and benzyl alcohol, with disproportionation of benzyl alcohol being of minor importance.

Functional-group reactivity

The versatility of the catalyst was investigated by testing the reactivity toward other functional groups in the benzylic position (Table 2). The secondary alcohol 1-phenylethanol was transformed into ethylbenzene in a yield of 57%, whereas the carbonyl compounds benzaldehyde and acetophenone underwent transfer hydrogenation and subsequent transfer HDO to form toluene and ethylbenzene in yields of 73 and 59%, respectively; furthermore, only trace amounts of styrene were observed from 1-phenylethanol and acetophenone. In the absence of a base, benzaldehyde dimethyl acetal was transformed into toluene in a yield of 61%. Benzoic acid was converted into the ester isopropyl benzoate under the reaction conditions; neither methyl benzoate nor benzyl isopropyl ether displayed any significant reactivity (Table 2, entries 5 and 6). Benzylamine and benzylmercaptan underwent transfer HDN and HDS in low and moderate yields, respectively (Table 2, entries 7 and 8), thus indicating that these reaction conditions might be applicable for the removal of benzylic thiol groups.

Table 2. Reactivity of functional groups in a benzylic position under the conditions optimised for the transfer HDO of benzyl alcohol.^[a]

Entry	Substrate	Product	Yield [%]
1	PhCH ₂ OH	PhCH ₃	93
2 ^[b]	PhCH ₂ OH		60
3	PhCHO		73
4 ^[b,c]	PhCH(OCH ₃) ₂		61
5	PhCOOCH ₃		≈ 0 ^[d]
6 ^[c]	PhCH ₂ OCH(CH ₃) ₂		8
7	PhCH ₂ NH ₂		13 ^[e]
8	PhCH ₂ SH		57
9	PhCH(OH)CH ₃	PhCH ₂ CH ₃	57
10	PhCH(O)CH ₃		59

[a] Unless otherwise noted, 100 mmol of substrate was used and the standard reaction conditions were employed with conversions of higher than 90%. [b] No Bu₄NOH was added. [c] An aliquot of 50 mmol of the substrate was added with 50 mmol of *para*-methylbenzyl alcohol. [d] The major product was isopropyl benzoate. [e] The conversion was 84%; the major product was not identified.

Hammett study

To gain further insight into the nature of the rate-determining step of the reaction, a Hammett study was carried out in line with earlier work^[27–30] (see the Experimental section for details). The Hammett study was conducted at a concentration low enough to ensure that disproportionation did not affect the result. A series of competition experiments were undertaken in which the relative rates for the transfer HDO of *para*-substituted benzylic alcohols to benzyl alcohol were determined. In a typical experiment, samples were extracted during the HDO of a mixture of 4 mmol of a *para*-substituted benzylic alcohol and 4 mmol of benzyl alcohol, and the reaction progress (i.e., the conversion of the benzylic alcohols) was determined by GC by using hexadecane as an internal standard. The *para*-substituted benzylic alcohols used were *para*-methylbenzyl alcohol, *para*-(methylthio)benzyl alcohol, *para*-chlorobenzyl alcohol, *para*-fluorobenzyl alcohol, and *para*-(trifluoromethyl)benzyl alcohol. *para*-Methoxybenzyl alcohol was excluded from the analysis as *para*-methoxybenzyl isopropyl ether was produced in addition to *para*-methoxytoluene.

In a competition study, the reaction order in each component will be the same for both substrates under the assumption that the substrates follow the same mechanism. Provided that the reaction is first order with respect to the substrate, the relative reactivities of the two benzylic alcohols can be determined by plotting $\ln(X_0/X)$ (where X is the concentration of the *para*-substituted benzylic alcohol and X_0 the initial concentration) against $\ln(H_0/H)$ (where H is the concentration of the benzyl alcohol and H_0 the initial concentration) (Figure 3). The relative reactivity k_{rel} was obtained as the slope of the line (Table 3).

The values of k_{rel} were used to construct the Hammett plot in Figure 4. Albeit none of the Hammett parameters provide a good correlation, σ^+ and the Creary constant σ_c^+ appear to show some correlation. The parameter σ_c^+ is based on the rate of the thermal rearrangement of methylenecyclopropanes to isopropylidenecyclopropanes. This reaction probes the stabiliz-

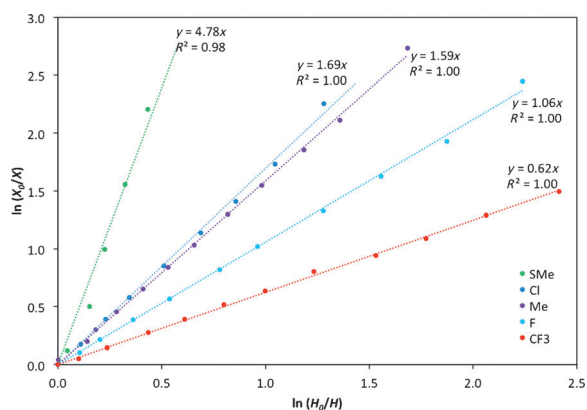


Figure 3. Kinetic data for competitive transfer HDO of benzyl alcohol and *para*-substituted benzylic alcohols.

Substituent	k_{rel}	σ	σ^+	σ_c^-
CF ₃	0.62	0.54	0.61	0.08
F	1.06	0.06	-0.07	-0.08
CH ₃	1.59	-0.17	-0.31	0.11
Cl	1.70	0.23	0.11	0.12
SCH ₃	4.78	0.00	-0.60	0.43

ing effect of various substituents on a benzylic radical-like transition state.^[31] This intriguing result led us to postulate that the transition state is dissimilar to the archetypical reactions used to determine the various sets of σ values and that DFT calculations could be used to shed more light on this aspect.^[32]

Computational studies

In an attempt to gain a deeper understanding of the mechanism of the transfer HDO, a theoretical study of the reaction was carried out by using DFT calculations in line with earlier studies.^[28,29,33-35] The interpretation of Hammett studies – and

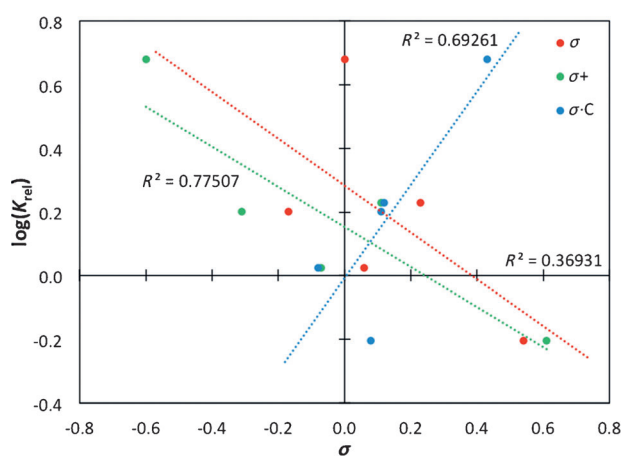


Figure 4. Hammett plot of $\log(k_{rel})$ versus σ , σ^+ , and σ_c^- values.

in particular nonlinear Hammett plots – can often be assisted by using computational chemistry.^[30] In particular, determination of the rate-determining transition state (TS) can shed light on the intrinsic details of the reaction mechanism.

The transfer HDO reaction is expected to proceed by initiation through the reduction of Mo^{VI} to Mo^{IV} by using *i*PrOH as the reductant, in line with reported results for the DODH reaction.^[9] Herein, we show that the Mo^{IV} moiety can oxidatively form a π -benzyl complex with the benzylic alcohol, which can undergo a reductive transfer hydrogenation, after isomerisation to a σ -benzyl complex, with concomitant reduction of Mo^{VI} to Mo^{IV}, thus closing the catalytic cycle of the reaction (Figure 5).

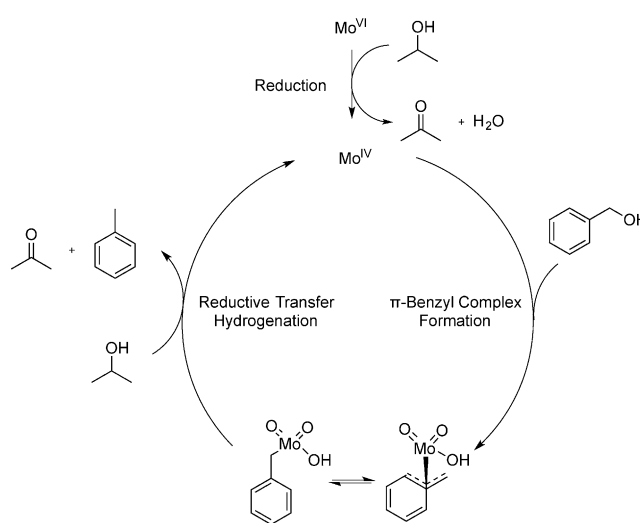


Figure 5. Tentative catalytic cycle for the Mo-catalysed transfer HDO reaction of PhCH₂OH with *i*PrOH as the reductant.

This mechanism is based on the well-known ability of molybdenum to form π -allyl and π -benzyl complexes.^[36-39] The first characterised η^3 -benzyl/metal complex $[(C_5H_5)(\eta^3-C_6H_5CH_2)Mo(CO)_2]$ was reported by King and Fronzaglia in 1966.^[40] Further evidence of this binding mode was reported by Cotton and LaPrade who reported the X-ray crystal structure of $[(C_5H_5)(\eta^3-p-MeC_6H_5CH_2)Mo(CO)_2]$.^[41] In addition to the bonding between the Mo centre and the benzylic C1 atom (2.269 Å), bonding between Mo and C2 and Mo and C3 (2.364 and 2.480 Å, respectively) was observed. Moreover, the C–C bond lengths of the four-carbon-atom segment C7–C6–C5–C4 approached that of a *cis*-1,3-butadiene group, thus suggesting some localisation of the π system.^[41] A variable-temperature NMR spectroscopic study of the same complex provided evidence of π - σ - π isomerisation of the benzyl ligand that occurs.^[42] Loss of aromaticity in the benzene ring is characteristic of η^3 -coordination in metal/benzyl complexes.^[38]

In the DFT calculations, which used the B3LYP-D3 functional and the LACVP** basis set, the molybdenum catalysts were treated as neutral complexes with oxide and hydroxide ligands. The calculations were carried out at atmospheric pressure at both 293.15 and 523.15 K (the latter is discussed herein and re-

ported in the Supporting Information; data for the calculations at 293.15 K are also available in the Supporting Information). We are aware of the strong acidity of $[H_2MoO_4]$ and, therefore, complemented our neutral model system with additional calculations involving charged species. A charged model system will suffer from incorrect charge distribution in DFT calculations, although modern solvation models might remedy this artefact to some degree. However, transition states were also modelled in the deprotonated state to assure that the charged species did not cause changes to the mechanistic pathway (see the Supporting Information for further details). Both $[MoO_3]$ and $[MoO_2(OH)_2]$ were considered as the starting moieties for the Mo^{VI} species, and the latter was found to be more stable, which corresponds to the reported results for $[CH_3ReO_2]$ versus $[CH_3ReO(OH)_2]$.^[43] This model system is based on the assumption that the heptamolybdate complex AHM will exist mainly as mononuclear molybdenum/oxo complexes at the high temperatures used. This assumption was in agreement with previous work that used the same model system, in which calculations showed higher Gibbs Free energies for the dinuclear complexes.^[7] In addition, the experimental results that used the mononuclear $[(Bu_4N)_2MoO_4]$ complex further supports this assumption. We ruled out the existence of molybdenum/hydride intermediates because the molybdenum/hydride complexes proved significantly less stable than the oxo complexes. In previous studies, reduction reactions with molecular hydrogen as the reductant were also proven to be energetically unfavourable.^[10]

The initial reduction from Mo^{VI} to Mo^{IV} is expected to go through coordination of *i*PrOH to the Mo^{VI} centre; furthermore, *i*PrOH coordinates as the *i*PrO⁻ ion and the proton is transferred to an oxo ligand. This coordination is followed by a reduction reaction, thus yielding a Mo^{IV} species, acetone, and water. The calculated energy profiles of these reactions are shown in Figure 6.

The pathway by complexation of *i*PrOH with $[MoO_3]$ [1–2] is favoured over complexation with $[MoO_2(OH)_2]$ by 4.5 [1'–2] and 14.5 kcal mol⁻¹ [1'–2'] (Figure 6). In addition, this pathway is also favoured at the reduction step because [2–3] is 14.5 kcal mol⁻¹ lower in energy than [2'–3].

With respect to the π -benzyl complex formation, two possible pathways were considered (Scheme 4). In pathway A, con-

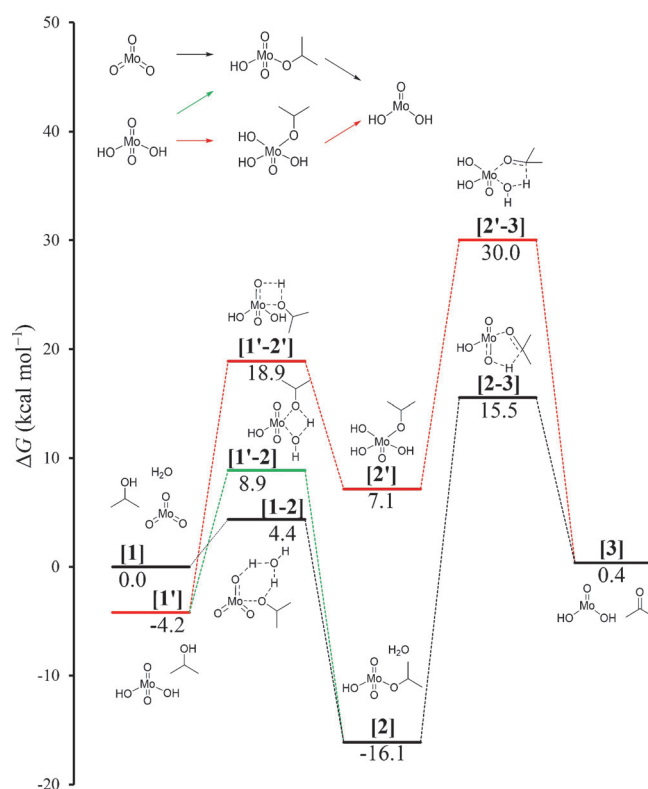
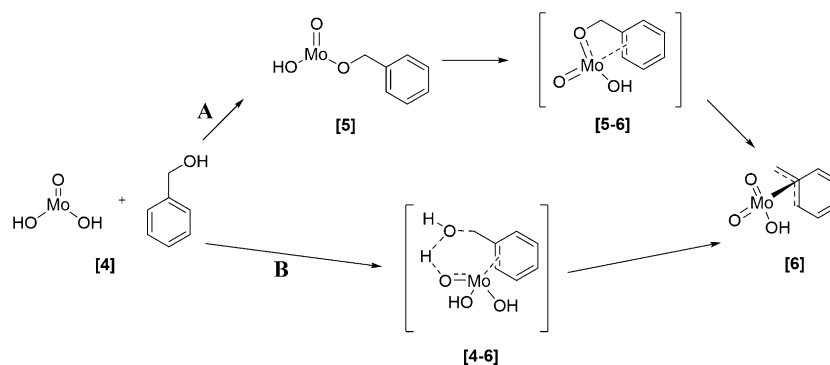


Figure 6. Calculated energy profiles for the reduction of Mo^{VI} to Mo^{IV} with *i*PrOH as the reductant.

densation of the Mo^{IV} moiety [4] with $PhCH_2OH$ gives [5], which was followed by a [2,3]-sigmatropic rearrangement to yield the π -benzyl complex [6]. In pathway B, direct reaction through transition state [4–6] with the expulsion of water yields the same π -benzyl complex [6].

The two energetic profiles for the generation of the Mo/σ -benzyl complex [7] show that the energy barrier for the oxidative rearrangement [5–6] is significantly lower than the [4–6] transition by 26.2 kcal mol⁻¹ (Figure 7). Further calculations showed that complex [6] would isomerise toward the σ -benzyl complex [7], thus leaving the molybdenum centre bonded to the CH_2 group through a σ bond. This isomerisation is driven by the energetically favourable re-aromatisation of the ben-



Scheme 4. The two investigated pathways for the formation of the Mo/π -benzyl complex.

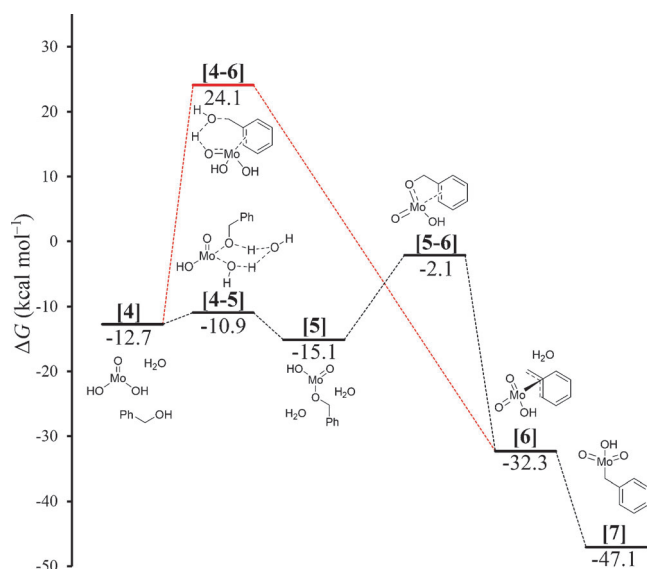


Figure 7. Calculated energy profiles for the oxidative generation of the Mo^{VI}/σ-benzyl complex.

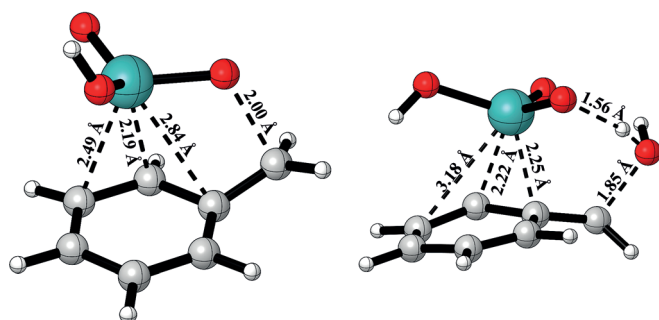
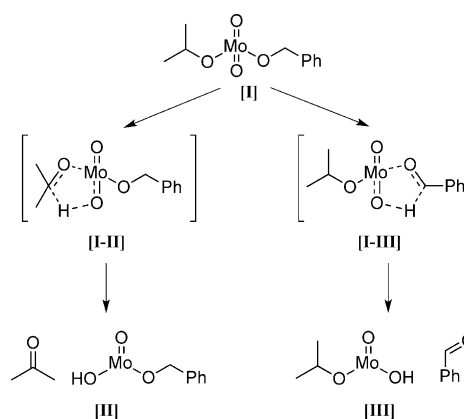


Figure 8. Transition states for the oxidative generation of the Mo/benzyl complex. Left: the favoured TS [5-6]; right: the disfavoured TS [4-6].

zene ring. The two transition states for the oxidative generation of the Mo/benzyl complex are shown in Figure 8.

The reduction of oxomolybdenum(VI) to oxomolybdenum(IV) by *i*PrOH can proceed as suggested previously,^[10] which upon subsequent coordination of PhCH₂OH results in the formation of intermediate [5]. An alternative mechanism is if the coordination of PhCH₂OH to the molybdenum centre took place prior to the oxidation of *i*PrOH, which would require an intermediate with both PhCH₂OH and *i*PrOH bonded to Mo^{VI} species [1]. However, for rhenium it has already been shown that benzyl alcohol can also be used as a reductant in this type of reduction reaction, thus yielding benzaldehyde.^[44] Calculations were carried out that used a transition state similar to [2-3] to differentiate between the oxidation of *i*PrOH and PhCH₂OH (Scheme 5).

The energy difference for the two different reduction pathways to [II] and [III] is only 0.3 kcal mol⁻¹ (the oxidation of PhCH₂OH is favoured), which shows that both pathways are possible and that the choice of pathway can be influenced by employing different concentrations (Scheme 5). Furthermore,



Scheme 5. Two possible oxidation pathways from a Mo^{IV} complex coordinated to benzyl alcohol and *i*PrOH.

this result explains why a small amount of benzaldehyde is observed, even when the transfer HDO of PhCH₂OH is conducted in *i*PrOH. Toward the end of the reaction, the formed PhCHO is presumably reduced to PhCH₂OH followed by the transfer HDO reaction; furthermore, this transfer hydrogenation is assumed to follow a Meerwein-Schmidt-Ponndorf-Verley (MSPV) mechanism with direct hydrogen transfer through a six-membered transition state.^[45] No change in the oxidation state of the catalyst is involved in this reaction; therefore, the oxidation state of the molybdenum species can be either +IV or +VI. Consequently, both pathways were calculated and showed similar energy barriers, namely, 37.3 and 37.0 kcal mol⁻¹ for Mo^{IV} and Mo^{VI}, respectively, relative to [2] and 20.9 and 21.1 kcal mol⁻¹, respectively, relative to [1]. These energies correlate well with previously calculated results for the aluminium-catalysed MSPV reductions, which were found to have transition-state energies of roughly 15–20 kcal mol⁻¹.^[45] These transition states are shown in Figure 9.

Deuterium-labelling experiments (see below) proved that the hydrogen transfer to toluene takes place reductively; that is, a hydride ion is transferred from the carbon atom in *i*PrOH rather than proton transfer from the oxygen atom. We suggest a complexation of *i*PrOH to the σ-benzyl complex [7], which can then undergo hydride transfer from the π complex, thus yielding toluene, acetone, and the Mo^{IV} moiety [MoO(OH)₂]. Direct transition from [7] to [9] was considered, but no feasible transition state could be found. The transition state for this hydride transfer is shown in Figure 11, and these two last steps (i.e., transition states [7-8] and [8-9]), with [4] as an end point have been added to a full-energy diagram of the catalytic cycle in Figure 10 (constructed from [4] because the previous steps serve as initiation). This conversion of benzyl alcohol and isopropanol into toluene, acetone, and water is exergonic by 37.4 kcal mol⁻¹, somewhat lower than the difference between [4] and [9] due to lower stabilisation from intermolecular bonding in [9].

Starting with the deprotonated species [MoO₂(OH)⁻], instead of [MoO(OH)₂], the energies of both the transition states and the intermediates of the catalytic cycle in Figure 10 were also determined (see Figure S11 in the Supporting Information). A

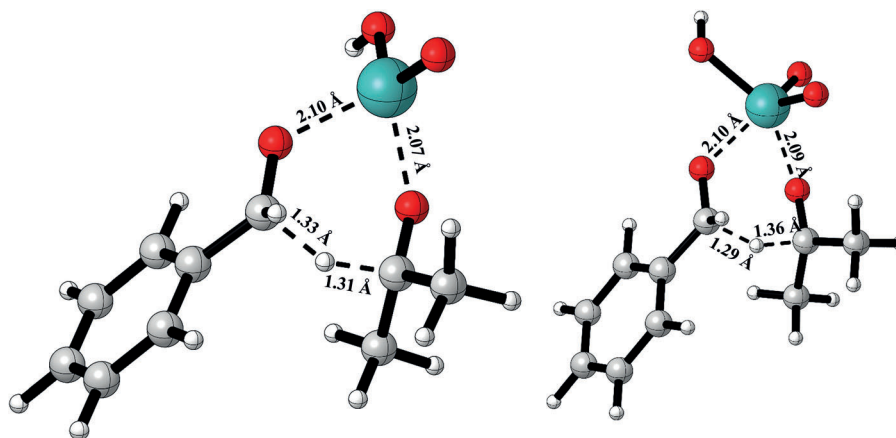


Figure 9. Transition states of the MSPV reduction catalysed by Mo^{IV} (left) and Mo^{VI} (right) species.

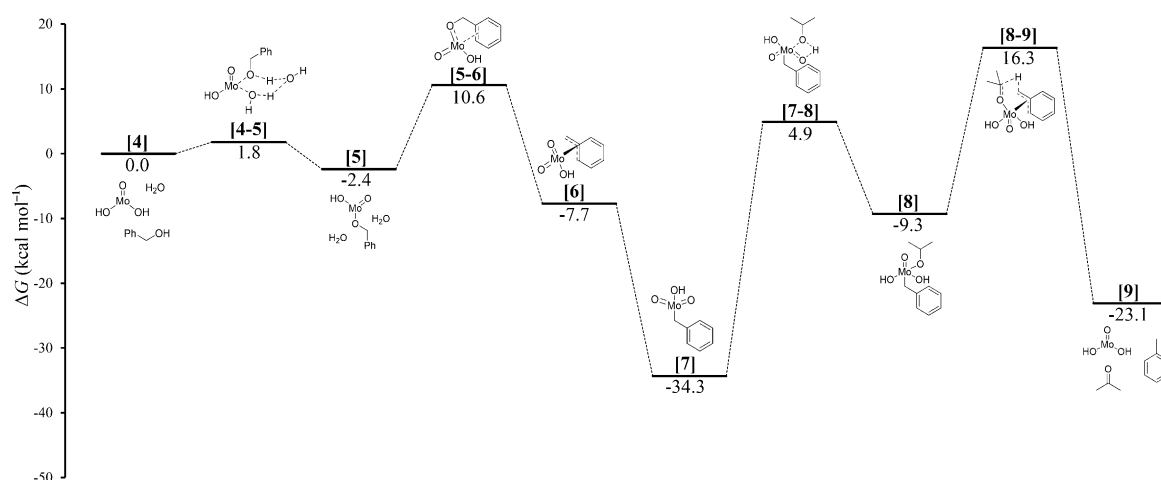


Figure 10. Energy profile for the proposed catalytic cycle for Mo-catalysed transfer HDO of benzyl alcohol with *i*PrOH as the reductant.

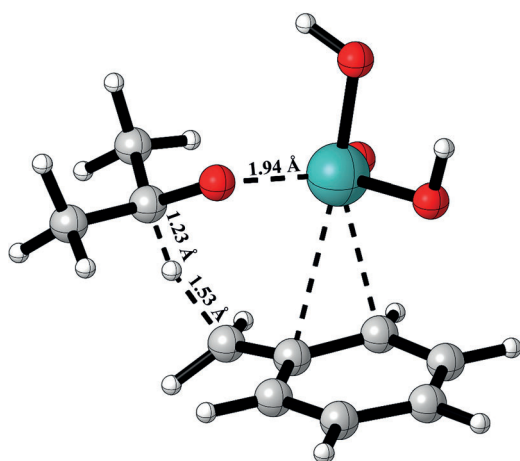


Figure 11. Transition state for the final hydride transfer ([8–9]).

good agreement between the two sets of calculations that used the charged and neutral catalytic species was observed, although the results differ in the stabilisation of the π com-

plexes ([6] in Figure 10 and Figure S11 in the Supporting Information), thus leading to an increase of 3.2 kcal mol⁻¹ in the energetic span of the reaction. Due to this increase, the neutral model system was used throughout the following calculations because this system was deemed to be the more probable.

For the final validation of this mechanism, the results from the Hammett study (Figure 4) were reconsidered in light of the proposed mechanism. The lack of linearity with any of the σ values shows that the Hammett study alone cannot be used to elucidate the reaction mechanism. The study can be used for validation of our computational calculations, thus examining the correlation between experiment and theory. Figure 10 shows transition state [8–9] to be the rate-determining step; therefore, the gap between [7] and this transition state constitutes the energetic span for the reaction. However, we note that [5–6] and [7–8] are also high in energy, and all these transition states were modelled for the various *para* substituents incorporated in the Hammett study to make certain that the rate-determining step does not switch for any of the *para* substituents. For an evaluation, the turnover frequencies (TOFs) for each mechanistic pathway were calculated by using the

AUTO program,^[46] and the relative TOF values gave a linear correlation when compared with the experimentally obtained relative reaction rates (Figure 12). The use of relative TOF values presents a method for dealing with reaction pathways with two or more rate-determining steps and also works in cases with only one rate-determining step for which the relative TOF value approaches the k_{rel} value.

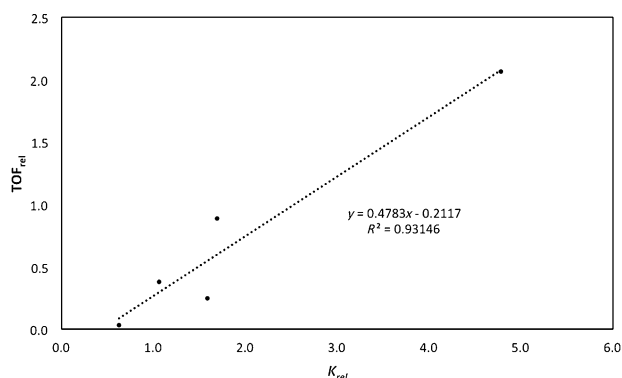


Figure 12. Correlation of the calculated relative TOF values with relative reactivities determined in the competition experiments (Hammett study).

The slope of the linear regression should equal one, but deviations are often observed when correlating theoretical and experimental results of the Hammett studies.^[33] However, the overall good correlation between experiment and theory for the proposed mechanism does not explain the nonlinearity observed in the Hammett study. Inspection of TS [5–6] and [8–9] demonstrates a significant loss in aromaticity in the benzene ring as a result of the π -benzyl bond (Figure 13). In TS [5–6], the C–C bonds of the benzene ring involved in the π -benzyl bond are elongated. In contrast, the C–C bond lengths of the benzyl ring in TS [8–9] alternate between longer and shorter bond values. We propose that the loss of aromaticity that leads to localisation of the π system results in the nonlinearity of the experimental Hammett studies because Hammett theory and correlation to σ values is only suitable for aromatic systems.

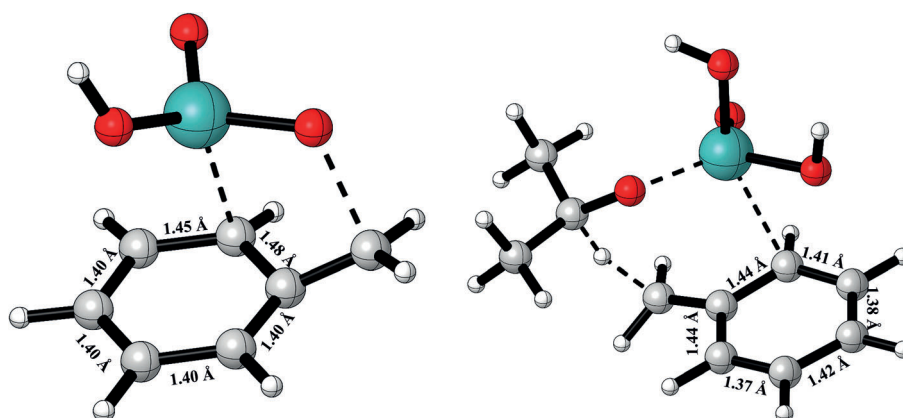


Figure 13. Loss of aromaticity in the benzyl ring (C–C bond lengths are shown). Left: TS [5–6]; right: TS [8–9].

Conclusions

The molybdate-catalysed transfer hydrodeoxygenation (HDO) reaction was investigated by using a combination of experimental and theoretical methods. A Hammett study that compared the relative rates for the transfer HDO of five *para*-substituted benzylic alcohols was shown not to correlate with a variety of σ values. We attribute this outcome to the significant loss of aromaticity of the benzyl ring in both TS [5–6] and [8–9], as demonstrated by using DFT calculations. The transfer HDO could also be carried out in neat PhCH₂OH at temperatures as low as 175 °C. Under these conditions, PhCH₂OH underwent disproportionation to yield benzaldehyde, toluene, and significant amounts of bibenzyl. Isotopic-labelling experiments (with PhCH₂OD and PhCD₂OH) showed incorporation of deuterium atoms into the resultant toluene that originated from the α position of benzyl alcohol, which is in line with the mechanism proposed by the DFT study. The increased mechanistic understanding of the molybdate-catalysed transfer HDO reported herein will be important for further expanding the scope of the reaction to form biomass-derived chemical building blocks.

Experimental Section

Standard reaction conditions

Substrate (441 mg, 100 mmol) [(NH₄)₆Mo₇O₂₄]·4H₂O (2.5 mol% of Mo), Bu₄NOH in MeOH (7.5 mL, 1 M), hexadecane as an internal standard (1 g), and *i*PrOH (150 mL) were mixed in a 400 mL Berghof autoclave with a magnetic stir bar (500 rpm) and a computer-controlled heating plate. The autoclave was sealed, pressurised with N₂ (15 bar), and heated to 250 °C for 8 h; the temperature typically stabilised between 240 and 250 °C, whereas the maximum pressure was 80–85 bar. The autoclave was sometimes equipped with a setup that allowed liquid sampling during the reaction. In these experiments, the volume of *i*PrOH was increased to 200 mL. The reaction mixture was analysed by means of GC for determination of the conversion and yields and by GC-MS for observation and identification of other products.

For reactions conducted at lower concentrations (4, 8, 20, and 50 mmol), the ratio of the reactants was kept constant, except for the volume of *i*PrOH. For example, if 20 mmol of benzyl alcohol was used, the quantity of AHM, 1 M Bu₄NOH in MeOH and hexadecane was divided by 5; however, 200 mL of *i*PrOH was still used.

Hammett study

The Hammett study was carried out as five separate competition experiments, in which a mixture of PhCH₂OH (4 mmol), a *para*-substituted benzylic alcohol (4 mmol), [(NH₄)₆Mo₇O₂₄]·4H₂O (35.4 mg, 2.5 mol% of Mo), Bu₄NOH in MeOH (0.6 mL of 1 M), hexadecane as an internal standard (80 mg), and *i*PrOH (200 mL) were mixed in a 400 mL Berghof autoclave with a magnetic stir bar (500 rpm) and a computer-controlled heating plate. The autoclave was sealed, pressurised with N₂ (15 bar), and heated to 250 °C for 7 h; the temperature typically stabilised between 240 and 250 °C. The autoclave was equipped with a setup that allowed liquid sampling during the reaction and samples were extracted at intervals of 20 min. The reaction mixture was analysed by means of GC for determination of the conversion and yields. By plotting ln(X₀/X) versus ln(H₀/H) (H and X are the concentrations of PhCH₂OH and the *para*-substituted benzylic alcohol at time *t*, respectively, and H₀ and X₀ are the same quantities at time *t*=0) a straight line with an intercept at *y*=0 and a slope equal to the relative rate of $k_{rel} = k_X/k_H$ was obtained.^[30] The Hammett plot was constructed by plotting log(*k*_{rel}) versus different sets of σ values.^[31, 47–50]

DFT calculations

DFT calculations were performed by using Jaguar^[51] with the B3LYP functional^[52, 53] and added D3 corrections.^[54] We used the LACVP** basis set, which applies the Hay–Wadt ECP and basis set for molybdenum, and the 6–31G** basis set for the other atoms.^[55] Transition states were found by using either a quadratic synchronous transit (QST) search^[56] or the standard transition-state search incorporated in the Jaguar suite. Intermediates were found by minimising the transition states toward both the expected starting material and the expected final product, thus confirming the correct transition state. The intermediates and transition states were characterised by carrying out full analytic frequency calculations at 293.15 and 523.15 K, which resulted in only positive frequencies for intermediates and exactly one imaginary frequency for the transition states. The calculations were performed at atmospheric pressure, and the reported values are given at 523.13 K (see the Supporting Information for the values calculated at 293.15 K). The transition states involving hydrogen transfer were modelled as both a direct transfer and as a transfer mediated through a water molecule. The transition state of the lowest energy is shown and the other transition state can be found in the Supporting Information. Approximate Gibbs free energies in the solution phase *G*_{solv} were obtained through the addition of the total Gibbs free energy (at 298.15 or 523.15 K) and the solvation energy ($E_{SCF, solv} - E_{SCF, gas}$) obtained through a single-point energy calculation with the Poisson–Boltzmann solver (PBF)^[57, 58] by using standard parameters for methanol (SCF: Self-Consistent Field). The computational model system was kept neutral to avoid complications when comparing the charged and neutral species computationally.^[59] We do not rule out the possibility of charged molecular species, but rather suggest that the neutral complexes treated in this study are suitable computational models of the actual complexes. The main mechanism was also modelled in its deprotonated state (see the Supporting Information for details). The visualisation and comparison of the structures were performed by using Maestro.^[60] The structural figures pre-

sented herein were created with CYLview using the POV raytracer for rendering.^[61]

Acknowledgements

This work was supported by a Sapere Aude research leader grant (P.F.) from the Danish Council for Independent Research, Grant 11-105487, and a grant from the Villum Foundation, Grant 341/300-123012.

Keywords: deoxygenation · density functional calculations · Hammett · homogeneous catalysis · molybdenum

- [1] J. R. Dethlefsen, P. Fristrup, *ChemSusChem* **2015**, *8*, 767–775.
- [2] S. Raju, M.-E. Moret, R. J. M. Klein Gebbink, *ACS Catal.* **2015**, *5*, 281–300.
- [3] J. R. Dethlefsen, P. Fristrup, *ChemCatChem* **2015**, *7*, 1184–1196.
- [4] C. Boucher-Jacobs, K. M. Nicholas, *Organometallics* **2015**, *34*, 1985–1990.
- [5] C. Boucher-Jacobs, K. M. Nicholas, *Top. Curr. Chem.* **2014**, *353*, 163–184.
- [6] S. Raju, J. T. B. H. Jastrzebski, M. Lutz, L. Witteman, J. R. Dethlefsen, P. Fristrup, M.-E. Moret, R. J. M. Klein Gebbink, *Inorg. Chem.* **2015**, *54*, 11031–11036.
- [7] L. Hills, R. Moyano, F. Montilla, A. Pastor, A. Galindo, E. Álvarez, F. Marchetti, C. Pettinari, *Eur. J. Inorg. Chem.* **2013**, 3352–3361.
- [8] J. R. Dethlefsen, D. Lupp, B.-C. Oh, P. Fristrup, *ChemSusChem* **2014**, *7*, 425–428.
- [9] D. Lupp, N. J. Christensen, J. R. Dethlefsen, P. Fristrup, *Chem. Eur. J.* **2015**, *21*, 3435–3442.
- [10] J. R. Dethlefsen, D. Lupp, A. Teshome, L. B. Nielsen, P. Fristrup, *ACS Catal.* **2015**, *5*, 3638–3647.
- [11] G. Chapman, K. M. Nicholas, *Chem. Commun.* **2013**, *49*, 8199–8201.
- [12] E. Furimsky, *Appl. Catal. A* **2000**, *199*, 147–190.
- [13] H. A. Wittcoff, B. G. Reuben, J. S. Plotkin, *Industrial Organic Chemicals*, Wiley, Hoboken, 3rd ed., **2013**.
- [14] P. M. Mortensen, J.-D. Grunwaldt, P. A. Jensen, K. G. Knudsen, A. D. Jensen, *Appl. Catal. A* **2011**, *407*, 1–19.
- [15] H. Wang, J. Male, Y. Wang, *ACS Catal.* **2013**, *3*, 1047–1070.
- [16] Y. Nakagawa, S. Liu, M. Tamura, K. Tomishige, *ChemSusChem* **2015**, *8*, 1114–1132.
- [17] A. Corma, O. de La Torre, M. Renz, N. Vollandier, *Angew. Chem. Int. Ed.* **2011**, *50*, 2375–2378; *Angew. Chem.* **2011**, *123*, 2423–2426.
- [18] S. Stanowski, K. M. Nicholas, R. S. Srivastava, *Organometallics* **2012**, *31*, 515–518.
- [19] A. D. Sutton, F. D. Waldie, R. Wu, M. Schlaf, L. A. P. Silks, J. C. Gordon, *Nat. Chem.* **2013**, *5*, 428–432.
- [20] N. Ota, M. Tamura, Y. Nakagawa, K. Okumura, K. Tomishige, *Angew. Chem. Int. Ed.* **2015**, *54*, 1897–1900; *Angew. Chem.* **2015**, *127*, 1917–1920.
- [21] T. Prasomsri, T. Nimmanwudipong, Y. Román-Leshkov, *Energy Environ. Sci.* **2013**, *6*, 1732–1738.
- [22] Y. Amada, N. Ota, M. Tamura, Y. Nakagawa, K. Tomishige, *ChemSusChem* **2014**, *7*, 2185–2192.
- [23] N. Ji, X. Wang, C. Weidenthaler, B. Spliethoff, R. Rinaldi, *ChemCatChem* **2015**, *7*, 960–966.
- [24] R.-J. van Putten, J. C. van der Waal, E. de Jong, C. B. Rasrendra, H. J. Heeres, J. G. de Vries, *Chem. Rev.* **2013**, *113*, 1499–1597.
- [25] B. L. Wegenhart, L. Yang, S. C. Kwan, R. Harris, H. I. Kenttämaa, M. M. Abu-Omar, *ChemSusChem* **2014**, *7*, 2742–2747.
- [26] G. R. Kasner, C. Boucher-Jacobs, J. M. McClain, K. M. Nicholas, *Chem. Commun.* **2016**, *52*, 7257–7260.
- [27] L. Keinicke, P. Fristrup, P.-O. Norrby, R. Madsen, *J. Am. Chem. Soc.* **2005**, *127*, 15756–15761.
- [28] P. Fristrup, M. Kreis, A. Palmelund, P.-O. Norrby, R. Madsen, *J. Am. Chem. Soc.* **2008**, *130*, 5206–5215.
- [29] I. S. Makarov, P. Fristrup, R. Madsen, *Chem. Eur. J.* **2012**, *18*, 15683–15692.

- [30] D. Lupp, N. J. Christensen, P. Fristrup, *Dalton Trans.* **2014**, *43*, 11093–11105.
- [31] X. Creary, M. E. Mehrsheikh-Mohammadi, S. McDonald, *J. Org. Chem.* **1987**, *52*, 3254–3263.
- [32] N. Christensen, P. Fristrup, *Synlett* **2015**, 508–513.
- [33] J. Mielby, A. Riisager, P. Fristrup, S. Kegnaes, *Catal. Today* **2013**, *203*, 211–216.
- [34] P. Fristrup, M. Tursky, R. Madsen, *Org. Biomol. Chem.* **2012**, *10*, 2569–2577.
- [35] C. Engelin, T. Jensen, S. Rodriguez-Rodriguez, P. Fristrup, *ACS Catal.* **2013**, *3*, 294–302.
- [36] V. S. Joshi, V. K. Kale, K. M. Sathe, A. Sarkar, S. S. Tavale, C. G. Suresh, *Organometallics* **1991**, *10*, 2898–2902.
- [37] S. H. Lin, G. H. Lee, S. M. Peng, R. S. Liu, *Organometallics* **1993**, *12*, 2591–2599.
- [38] B. M. Trost, L. C. Czabaniuk, *Angew. Chem. Int. Ed.* **2014**, *53*, 2826–2851; *Angew. Chem.* **2014**, *126*, 2868–2895.
- [39] H. Teruel, N. Romero, I. Henriquez, *Transition Met. Chem.* **1995**, *20*, 426–429.
- [40] R. B. King, A. Fronzaglia, *J. Am. Chem. Soc.* **1966**, *88*, 709–712.
- [41] F. A. Cotton, M. D. LaPrade, *J. Am. Chem. Soc.* **1968**, *90*, 5418–5422.
- [42] F. A. Cotton, T. J. Marks, *J. Am. Chem. Soc.* **1969**, *91*, 1339–1346.
- [43] X. Li, D. Wu, T. Lu, G. Yi, H. Su, Y. Zhang, *Angew. Chem. Int. Ed.* **2014**, *53*, 4200–4204; *Angew. Chem.* **2014**, *126*, 4284–4288.
- [44] C. Boucher-Jacobs, K. M. Nicholas, *ChemSusChem* **2013**, *6*, 597–599.
- [45] R. Cohen, C. R. Graves, S. T. Nguyen, J. M. L. Martin, M. A. Ratner, *J. Am. Chem. Soc.* **2004**, *126*, 14796–14803.
- [46] S. Kozuch, *WIREs Comput. Mol. Sci.* **2012**, *2*, 795–815.
- [47] C. Hansch, A. Leo, R. W. Taft, *Chem. Rev.* **1991**, *91*, 165–195.
- [48] C. Hansch, H. Gao, *Chem. Rev.* **1997**, *97*, 2995–3060.
- [49] L. M. Stock, H. C. Brown, *Adv. Phys. Org. Chem.* **1963**, *1*, 35–154.
- [50] H. C. Brown, D. P. Kelly, M. Periasamy, *Proc. Natl. Acad. Sci. USA* **1980**, *77*, 6956–6960.
- [51] Schrödinger Release 2015–2012: Jaguar, version 8.8, Schrödinger, LLC, New York, NY, **2015**.
- [52] A. D. Becke, *J. Chem. Phys.* **1993**, *98*, 5648–5652.
- [53] A. D. Becke, *J. Chem. Phys.* **1993**, *98*, 1372–1377.
- [54] S. Grimme, J. Antony, S. Ehrlich, H. Krieg, *J. Chem. Phys.* **2010**, *132*, 154104–154122.
- [55] P. J. Hay, W. R. Wadt, *J. Chem. Phys.* **1985**, *82*, 299–310.
- [56] T. A. Halgren, W. N. Lipscomb, *Chem. Phys. Lett.* **1977**, *49*, 225–232.
- [57] D. J. Tannor, B. Marten, R. Murphy, R. A. Friesner, D. Sitkoff, A. Nicholls, B. Honig, M. Ringnalda, W. A. Goddard, *J. Am. Chem. Soc.* **1994**, *116*, 11875–11882.
- [58] B. Marten, K. Kim, C. Cortis, R. A. Friesner, R. B. Murphy, M. N. Ringnalda, D. Sitkoff, B. Honig, *J. Phys. Chem.* **1996**, *100*, 11775–11788.
- [59] P. Fristrup, M. Ahlquist, D. Tanner, P.-O. Norrby, *J. Phys. Chem. A* **2008**, *112*, 12862–12867.
- [60] Schrödinger Release 2015–2012: Maestro, version 10.2, Schrödinger, LLC, New York, NY, **2015**.
- [61] CYLview, 1.0b, C. Y. Legault, Université de Sherbrooke, **2009**, <http://www.cylview.org>.

Received: June 25, 2016

Published online on ■ ■ ■, 0000

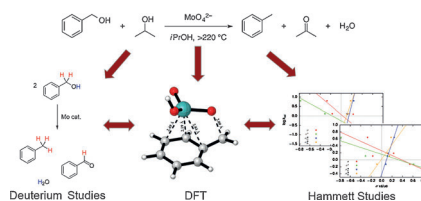
FULL PAPER

Homogeneous Catalysis

*D. B. Larsen, A. R. Petersen,
J. R. Dethlefsen, A. Teshome, P. Fristrup**



Mechanistic Investigation of Molybdate-Catalysed Transfer Hydrodeoxygenation



What a reduction! The molybdate-catalysed transfer hydrodeoxygenation (HDO) of benzyl alcohol to toluene has been investigated by using a combination of experimental and computational methods. A Hammett study and DFT calculations suggest a transition state with significant loss of aromaticity (see picture). Isotopic-labelling experiments show the incorporation of deuterium, which is in line with the mechanism suggested by the DFT study.